HHS Public Access

Author manuscript

Oncogene. Author manuscript; available in PMC 2015 November 07.

Published in final edited form as:

Oncogene. 2015 May 7; 34(19): 2483–2492. doi:10.1038/onc.2014.192.

Polyoma small T antigen triggers cell death via mitotic catastrophe

Arun T Pores Fernando[1,2,6], **Shaida Andrabi**[1,6,7], **Onur Cizmecioglu**[1,2], **Cailei Zhu**[3], **David M. Livingston**[1], **Jonathan M.G Higgins**[3,5], **Brian S Schaffhausen**[4], and **Thomas M Roberts**[1,2]

[1]Department of Cancer Biology, Dana-Farber Cancer Institute

[2]Department of Biological Chemistry and Molecular Pharmacology, Harvard Medical School, Boston, Massachusetts

[3]Division of Rheumatology, Immunology and Allergy, Brigham and Women's Hospital

[4]Department of Developmental, Molecular and Chemical Biology, Tufts University School of Medicine, Boston, Massachusetts

[5]Institute for Cell and Molecular Biosciences, Newcastle University, Newcastle-upon-Tyne, United Kingdom

Abstract

Polyoma small T antigen (PyST), an early gene product of the polyoma virus, has been shown to cause cell death in a number of mammalian cells in a protein phosphatase 2A (PP2A)-dependent manner. In the current study, using a cell line featuring regulated expression of PyST, we found that PyST arrests cells in mitosis. Live-cell and immunofluorescence studies showed that the majority of the PyST-expressing cells were arrested in prometaphase with almost no cells progressing beyond metaphase. These cells exhibited defects in chromosomal congression, sister chromatid cohesion and spindle positioning, resulting in the activation of the Spindle Assembly Checkpoint (SAC). Prolonged mitotic arrest then led to cell death via mitotic catastrophe. Cell cycle inhibitors that block cells in G1/S prevented PyST-induced death. PyST-induced cell death that occurs during M is not dependent on p53 status. These data suggested, and our results confirmed that, PP2A inhibition could be used to preferentially kill cancer cells with p53 mutations that proliferate normally in the presence of cell cycle inhibitors.

Keywords

apoptosis; cancer; DNA tumor virus; PP2A inhibition

Corresponding Authors: Drs. Thomas M. Roberts and Shaida Andrabi, Departments of Cancer Biology and Biological Chemistry and Molecular Pharmacology, Dana-Farber Cancer Institute, Harvard Medical School, 44 Binney Street, Boston, MA 02115. Phone: 617-632-3049; Fax: 617-632-4770; thomas_roberts@dfci.harvard.edu or shaida.andrabi@kashmiruniversity.ac.in.

[6]A T Pores Fernando and S Andrabi contributed equally to this work.

[7]Current address for S Andrabi, Department of Biochemistry, University of Kashmir, Kashmir, India

Conflict of Interest: The authors declare no conflict of interest.

Introduction

Murine polyoma virus, a small DNA tumor virus, encodes three early gene products- large T (PyLT), middle T (PyMT), and small T (PyST) (see [1] for a comprehensive review). Studies on polyoma viruses have long focused on the host cell proteins that are bound by the various early gene products. Thus, p53 and pRb were either first recognized or first studied via their interactions with SV40 LT [2, 3], while PI3 kinase was first studied via its interaction with PyMT [4]. A key binding protein for PyST is the protein phosphatase, PP2A [5]. Previous work from our lab and others has shown that much of the functionality of both PyST and SV40 ST (SVST) is dependent on their ability to bind to PP2A [5, 6].

PP2A is a serine-threonine phosphatase that has been implicated in the regulation of multiple signaling pathways regulating tumor suppression, mitosis and cell death [7-11]. Majority of the PP2A complexes exist as heterotrimeric complexes composed of a scaffolding A subunit (Aα or Aβ), a catalytic C subunit (Cα or Cβ), and a regulatory B subunit. However, a smaller fraction can exist as dimeric complexes (reviewed in [12]). Since there are multiple families of B subunits (B, B′, B″ or B‴ family members), PP2A can exist as more than 80 different complexes [8, 13]. ST antigens bind to PP2A-A subunits and replace B subunits in the enzyme complex, thereby modulating PP2A function. PyST can bind either PP2A-Aα or Aβ, while SVST antigen can only bind PP2A-Aα [14, 15].

Previously we showed that PyST can either induce or prevent apoptosis depending on what other signals the cell is receiving [15, 16]. Under normal growth conditions in the presence of serum, we found that expression of PyST via retroviral infection induces apoptosis in murine fibroblasts [16]. Notably, SVST expressed via the same vector fails to cause apoptosis under the same conditions [16]. We went on to demonstrate that there are other major differences between SVST and PyST in their effects on differentiation, transformation, and cell survival [15]. However, PyST expression decreased with cell passaging (due to death-associated cell drop-out), thereby hindering our efforts to characterize PyST mediated cell death [16].

In this report, we describe the engineering of a cell line featuring regulated expression of PyST and show that PyST-mediated cell death occurs during cell division and that p53 is dispensable for this process. PyST expression triggers chromosome alignment defects. The SAC checkpoint cannot be satisfied, arresting cells at, or prior to, metaphase. Prolonged mitotic arrest leads to mitotic catastrophe-associated cell death. Arresting cells prior to cell division protects them from PyST-mediated cell death. Harnessing this data, we show that PP2A inhibition can be used to selectively kill cancer cells that are resistant to cell cycle arrest such as those with deregulated p53 function.

Results

PyST triggers mitotic arrest

Constitutive PyST expression is toxic to cells and PyST levels decreases with cell passaging, thereby complicating further characterization of PyST induced cell death [16]. To overcome this, we constructed a U2OS osteosarcoma cell line in which PyST expression is under the

control of a tetracycline-regulated promoter system, to allow regulated protein expression. Western blotting revealed that protein expression was tightly regulated, and high levels of PyST expression were observed upon dox treatment (Supplementary Figure 1A). In addition, using immunofluorescence, we observed that PyST was found in the cytoplasm and in the nucleus, as has been seen in previous studies [17] (Supplementary Figure 1Aii).

Notably, there was an increase in the proportion of round, refractile cells following PyST expression, a phenotype associated with mitotic cells. This change was observable after 8h of protein expression and peaked at about 30h (Figure 1Ai), suggesting that PyST expressing cells may be arrested in mitosis. After 30h of PyST expression, we fixed and stained PyST expressing and control U2OS cells with propidium iodide and analyzed samples with flow cytometry. DNA content analysis revealed that more than 60% of the PyST expressing cells were in the G2 or M phases, compared to less than 15% for the control cells (Figure 1Aii). Treating cells with okadaic acid (OA), a well-known PP2A inhibitor, elicited similar results, as has been reported in the literature ([18] and data not shown). Immunofluorescence micrographs of mitotic markers such as phosphohistone H3 and cyclin B (Figure 1Bi) showed that a majority of the PyST expressing cells were in the mitotic phase of the cell cycle. Similarly, Western blotting demonstrated that PyST expressing cells had higher levels of late G2 to M cell cycle markers such as phosphorylated aurora kinase (AUK) and phosphorylated polo-like kinase1 (PLK1) (Figure 1C). Similar results were obtained with murine NIH 3T3 cells (Supplementary Figure 2).

PyST expressing cells are blocked prior to chromosome congression

We sought to determine at which stage in mitosis the PyST expressing cells were arrested. To this end, we expressed histone H2B-GFP in the inducible PyST-expressing cells and performed time-lapse imaging experiments in both the uninduced and PyST expressing conditions. Uninduced cells progressed normally through the cell cycle, with cells spending on average between 30 to 60 minutes in mitosis, as observed by chromosome condensation and nuclear breakdown, followed by alignment of the chromosomes at the metaphase plate, segregation of the chromosomes to the poles in anaphase, and finally, cytokinesis (Figure 2A and Movie 1). In contrast, the majority of the PyST expressing cells did not progress beyond metaphase. PyST expressing cells were blocked in mitosis for prolonged periods (ranging between 300-1200 minutes following nuclear envelope breakdown) (Figure 2B, C and Movie 2,3). PyST expressing cells failed to align their chromosomes at the metaphase plate. Even in cases where most of the chromosomes seemed to be aligned at the metaphase midplate, after a brief metaphase arrest, cells scattered their chromosomes and regressed to a prometaphase-like state, with their chromosomes tumbling along the mitotic spindle (Figure 2C and movie 3). Okadaic acid treatment also triggered a similar prometaphase-like mitotic arrest, with cells tumbling along the spindle axis (Supplementary Figure 3 and movie 4). In an alternative approach to obtain high-resolution data, we fixed control cells and cells expressing PyST and stained them with DAPI and pan phospho-aurora kinase. The persistence of pan phospho-aurora kinase staining in PyST expressing cells confirmed that these cells were still in mitosis (Figure 3A). Control cells displayed a normal cell cycle distribution with the majority of the cells in interphase. Control mitotic cells showed roughly equal proportions of mitotic cells in prometaphase (∼34%), metaphase (∼34%) and

anaphase and telophase combined (32%) (Figure 3B). However, a majority of the PyST expressing cells were in mitosis, predominantly arrested in a prometaphase-like state (∼90%) (Figure 3Bii). Moreover, only a small proportion of these cells were observed to have their chromosomes aligned at the metaphase plate (∼10%) and almost no cells were seen in anaphase (Figure 3B).

PyST expressing cells exhibit aberrant spindle formation, premature chromatid separtation and spindle checkpoint activation

We next used α- and γ- tubulin immunostaining to assess the status of the mitotic spindles. There was an increase in the incidence of multipolar spindle formation in PyST expressing cells (30% in PyST expressing cells compared to 3% in control cells), which correlated with the failure of chromosome alignment, while control cells had normal bipolar spindles (Figure 4A). In general, the spindle axis is thought to lie parallel to the substratum (reviewed in [19]). However, we observed that PyST expressing cells frequently contained misaligned spindle axes. Images of γ-tubulin staining for different z-stacks (0.3 microns intervals) were obtained and the orientation of the mitotic spindle in relation to the coverslip was determined. While we were able to observe both the spindle poles of the control cells on the same z plane (or very close to each other), they were frequently represented in different z planes for PyST expressing cells that had bipolar spindles. Since PyST-expressing cells contained misaligned chromosomes, we also asked whether they had lost their centromeric cohesion. We prepared mitotic chromosome spreads for control and PyST expressing U2OS cells and co-stained with anti-centromere antibodies and Hoechst 33342 for DNA visualization. In control cells only ∼5% of the cells had lost cohesion while in PyST expressing cells almost 60% exhibited separated or completely scattered sister chromatids (Supplementary Figure 4, Figure 4C).

Finally, we tested whether the spindle assembly checkpoint (SAC) had been triggered. As expected for prometaphase arrested cells, PyST expressing cells contained higher levels of phosphorylated checkpoint proteins, Bub1 and BubR1, than control cells as detected by Western blotting (Figure 5A). PyST expressing cells also showed characteristic Bub1 and BubR1 staining associated with SAC activation at the kinetochores (Figure 5B)[20, 21]. Consistent with these data, SAC override, achieved by treating PyST expressing cells with an inhibitor of MPS-1 [22], a dual-specificity kinase required for proper functioning of the SAC, rescued cells from G2/M cell cycle arrest (although the cells died in subsequent cell division cycles; data not shown). These results reveal that PyST-expressing cells are defective in their ability to align chromosomes at the metaphase plate, and that they possess aberrant mitotic spindles. Failure to align chromosomes on a normal biploar spindle and the resulting failure to satisfy the SAC in these cells leads to prolonged mitotic arrest.

PyST kills cells during cell division via mitotic catastrophe mediated apoptosis

The mitotic arrest caused by expression of PyST for 30 h was followed by cell death. FACS analysis at 40 hours showed that more than 60% of the PyST expressing cells were in the sub G1 cell population (compared to ∼3% for control cells (Figure 6A). Similarly, apoptosis was elevated in PyST-expressing cells as indicated by an increase in fragmented DNA (Figure 6B). To further characterize cell death, and to confirm that PyST mediated cell death

involved poly-ADP-ribose polymerase (PARP) activation [16], we analyzed total PARP levels via western blotting in lysates harvested from control U2OS cells and U2OS cells expressing PyST. PyST expressing cells showed significantly higher levels of cleaved PARP compared to control cells, consistent with the induction of apoptosis (Figure 6C). To determine the mode of cell death, we performed live-cell imaging in PyST expressing cells. As noted earlier, a majority of the PyST expressing cells were arrested in mitosis. Prolonged attempts at chromosome alignment at the metaphase plate were not successful, and cells ultimately died while still being trapped in mitosis (Figure 6D and Movie 5). These cells displayed characteristic apoptotic morphological features such as membrane blebbing, cell shrinkage and DNA condensation (Figure 6D and Movie 5). There was no detectable exit from mitosis. Notably, the apoptotic effects induced by PyST expression, could be negated by treating cells with aphidicolin, etoposide, or hydroxyurea - molecules that inhibit DNA synthesis and arrest cells in S phase (Figure 6E). This is consistent with our observations that cell death occurs in mitosis.

As an independent test to confirm that PyST induces apoptosis in G2/M, we expressed a fusion protein in which PyST was fused at its COOH terminus to “degrons”, which resulted in its destruction at certain phases of the cell cycle ([23] and Naetar et al., manuscript under review). After 50h of PyST expression, cells were either fixed and stained with crystal violet, or were analzyed by western blotting for PARP cleavage (Figure 6F). Notably, PyST fused to a geminin degron, which caused its destabilization outside of the G2/M phases, triggered cell death in U2OS osteosarcoma cells, while a PyST fused to a cdt1 degron, which caused its destruction outside of the G1 phase, was unable to kill (Figure 6F). Taken together, the data indicate that PyST-mediated cell death occurs via mitotic catastrophe-associated apoptosis.

PyST mediated cell death is independent of p53 status and PP2A inhibition can be manipulated to preferentially kill p53 deregulated cancer cells

Since the U2OS cells we had been using express wild type p53, we tested whether PyST-mediated cell death is p53-dependent. Both parental U2OS cells and isogenic U2OS cells expressing a dominant negative allele of p53 (ddp53) were sensitive to PyST-mediated cell death, indicating that p53 is dispensable for this process (Figure 7A). Human H1299 cells, which are p53 null, were also sensitive to PyST induced cell death (Figure 7A). Although PP2A inhibitors such as OA have been considered as potential anti-tumor therapeutics, they are lethal to both tumor cells and normal cells alike. This is also true for PyST, which kills both tumor cells and non-neoplastic cells such as HMEC and NIH3T3. However, as shown above, cells are protected from PyST induced cell death, when they are arrested by cell cycle inhibitors or DNA damaging agents shown to trigger cell cycle arrest in wild type p53 cells [24]. Since death mediated by PP2A inhibition did not require p53, we explored the possibility of selectively killing p53 null tumor cells while relying on the p53 in wild type host cells to spare them via p53- mediated growth arrest [25]. To this end, we tested whether treatment of cells with a DNA damaging drug, such as etoposide, would arrest cells that synthesize and activate wild type p53 and spare them from a PP2A inhibitor, while allowing p53 null cells to die.

Wild type p53 U2OS cells and U2OS cells expressing dominant negative p53 (ddp53) were seeded at low density and cultured till they reached about 60-80% confluence (∼ 3 days) in the presence of a low dose of etoposide (150 nM). Etoposide treatment slowed the proliferation rate of wild type U2OS cells, eventually forcing them into cell cycle arrest, while the cells expressing ddp53 were not affected. Following this treatment, the cells were treated with 15 nM okadaic acid for 48 hours in the presence of etoposide. Okadaic acid treatment triggered mitotic arrest and subsequent cell death in cells expressing ddp53 compared to the p53 wild type cells that were arrested by etoposide treatment (Figure 7B). Cells were then allowed to recover and cell density was measured via crystal violet staining (Figure 7B). Okadaic acid treatment killed ∼75% of the ddp53 expressing cells compared to ∼20% of normal cells (Figure 7Bii). We also performed similar experiments in MCF10 A cells, a non tumorigenic human epithelial cell line, to determine if similar results were obtained with other chemical inhibitors. MCF10 A cells and MCF10 A cells expressing ddp53 were treated with 200 nM aphidicolin for 4∼5 days and then treated with 1.5 μM cantharidin- a PP2A inhibitor for 18∼20 hours. Cells were then allowed to recover and cell density was measured via crystal violet staining (Figure 7C,D). Cantharidin treatment killed ∼50% of the ddp53 expressing MCF10 A cells compared to ∼7% of normal cells when coupled with aphidicolin treatment (Figure 7C).

Discussion

Polyoma and SV40 T antigens have long been associated with tumorigenesis, usually driving cell cycle progression via their interactions with host cell proteins. Various combinations of T antigens along with activated oncogenes have regularly featured in the recipes for engineering tumor cells from primary cells (reviewed in [1, 26]). Here we show that PyST, rather than driving cell cycle progression, instead mediates cell death during mitosis, and that p53 is dispensable for this process. PyST expressing cells fail to properly align their chromosomes at the metaphase plate, preventing progression to anaphase. Prolonged mitotic arrest leads to mitotic catastrophe-associated apoptosis. Notably, our studies of PyST associated apoptosis have suggested a way to use PP2A inhibitors to kill p53 mutant tumor cells while sparing cells with normal p53.

Live-cell imaging of PyST expressing cells showed that cells that had reached partial metaphase alignments eventually reverted back to a prometaphase-like state, with their chromosomes tumbling along the mitotic spindle. There are a number of potential explanations for these results. One possibility is that the separation of sister chromatids observed when PyST is expressed (Figure 4) prevents chromosome bi-orientation and triggers prometaphase arrest [27]. This could be caused by an inappropriate release of cohesin, which holds chromatids together. Indeed, PP2A along with shugoshin plays a critical role in the protection of cohesion at centromeres during mitosis [28-30]. However, our results do not necessarily implicate PyST in affecting cohesion through PP2A and Sgo1 because cohesion fatigue as an indirect result of prolonged mitotic arrest could also underlie our observations [27]. In either case, loss of spindle pole integrity as a consequence of failed chromosome cohesion may also explain the increase in incidence of multipolar spindle formation[31]. Additional experiments are needed to test the direct effect of PyST on Sgo1 and cohesion.

There are other factors that could also contribute to the observed mitotic arrest. Kinetochore fibers (K-fibers), a subset of microtubules that orchestrate chromosome alignment during mitosis, require the activity of PP2A (B56-PP2Acomplex) for their stability [32]. Preliminary data suggest that a proportion of PyST expressing cells have thinner K-fibers (data not shown). This could lead to unstable kinetochore microtubule attachment, thereby resulting in SAC activation and mitotic arrest. Defects in spindle positioning (Figure 4B) might also lead to delays in mitotic progression [33].

ST has been observed to either augment or diminish PP2A phosphatase activity [15, 34-36]. Interestingly, both inhibitors (such as okadaic acid) and activators (specifically FTY720) of PP2A have shown promise in killing particular tumor types [37, 38]. However, it seems reasonable to hypothesize that the mitotic arrest induced by PyST in the inducible cells that we have characterized results from its ability to inhibit PP2A. Notably, okadaic acid treatment has also been shown to trigger mitotic arrest ([18] and presented here). While we are confident that the effects we see with PyST and okadaic acid are mediated via PP2A inhibition (PP2A binding defective PyST mutant does not kill cells [16] and PP2A A-beta inhibition kills cells [39]); contributions by other phosphatases cannot be completely ruled out. Interactions of ST with other phosphatases have not been tested and okadaic acid, and cantharidin can inhibit other phosphatases such as PP1, PP4 and PP5 [40, 41]. We are in the process of deciphering which B subunit knockdown could mimic PyST mediated mitotic defects. The levels of PyST that we see expressed via regulated expression in the present report are much greater than those achieved via constitutive expression in our previous reports[15, 16]. This is likely a result of progressive elimination from the culture of dying cells resulting from stable expression of PyST at any but the lowest levels.

Indeed, there are a few differences in the modes of cell death mediated by constitutive low PyST expression levels, compared to regulated high PyST expression levels. For example, we saw caspase activation associated with the cell death mediated by regulated PyST expression (data not shown) but not with the apoptosis brought about constitutive expression[16]. Thus, there could be multiple modes of PyST mediated killing, based on the amount of PyST expressed. Interestingly, adenoviral overexpression of SV40 ST also results in very high levels of expression, and has also been reported to trigger mitotic arrest in fibroblasts. [42] Notably cell death mediated by high levels of SVST is also p53 independent [43]. Recent studies from the Branton group demonstrated a similar phenotype with the overexpression of adenoviral E4orf4 protein, another viral protein known to inhibit PP2A function [44, 45]. However, these two viruses differ in their mode of action; E4orf4 binds to PP2A B subunits [44] while both SVST and PyST replace B subunits. We hypothesize that high levels of each of these proteins function like a wrench in the gears of PP2A, inhibiting its function in an okadaic-acid like manner. Notably, lower levels of expression of SVST and/or E4orf4 did not lead to mitotic catastrophe, or indeed to apoptosis. In contrast, even low levels of expression of PyST causes mitotic arrest and cell death (Supplementary Figure 5). In this case, PyST may be acting to selectively target PP2A to one or more mitotic targets. Indeed, when we performed affinity purification of PyST complexes a number of mitotic proteins were selectively pulled down (unpublished observation). It is possible that the PyST-mediated block in mitosis is regulated by its ability to control phosphorylation of these and or other mitotic proteins resulting in either their

overphosphorylation at high levels of PyST expression or underphosphorylation at low levels of PyST expression. Currently, we are examining how these binding proteins contribute to the development of cellular features characteristic of PyST mediated mitotic blockage.

We have been struck by how toxic both OA and PyST are to tumor cells. However, while this is good news in that few cells would likely survive either agent to become resistant, both agents are clearly toxic to normal cells. In the current study, we show that polyoma ST mediated cell death is independent of p53 status. This result is consistent with the previous finding from the Fried lab that PyST can overcome a strong p53 block to PyMT transformation of REF52 cells [46, 47]. Since p53 is not required for PyST- or OA-mediated cell death, we were able to exploit this property to use OA and other less toxic PP2A inhibitors to preferentially kill p53-deregulated cancer cells. This same trick, using DNA damaging agents to instigate cell cycle arrest in normal cells has been utilized by others to increase the therapeutic window of other compounds that attack the cell cycle machinery to cause cell death in mitosis (reviewed in [25, 37, 48, 49]) and we have extended this to PP2A inhibition. We also propose that more specific PP2A inhibitors that target a single PP2A complex involved in mitosis, or a subset of PP2A complexes, such as those that only target PP2A A-beta specific complexes, are likely to be more effective in cancer therapy. Currently, we are in the process of identifying novel PP2A substrates that regulate mitosis, as these could serve as attractive therapeutic targets.

Materials and Methods

Materials

Anti α-tubulin, doxycycline, crystal violet and cantharidin were purchased from Sigma. Anti γ-tubulin and phospho Plk1 antibodies were purchased from Biolegend. Antibodies against pan phospho aurora kinase, HA, phospho histone3 (Ser 10) and cyclin B were purchased from Cell Signaling Technology. Anti-BubR1 antibody was purchased from BD Biosciences, and centromere autoantibodies were purchased from Immunovision. Secondary FIT-C and TRIT-C antibodies were obtained from Jackson Immunoresearch Laboratories. Secondary Alexa 488 and Alexa 568 were obtained from BD Biosciences. Aphidicolin, hydroxyurea, etoposide and okadaic acid were obtained from Calbiochem. pTREX plasmid was a gift from Novartis Pharmaceuticals. PyST was cloned in the pTREX plasmid using standard molecular biology techniques. Dominant negative p53 (pWZL-p53DD) was a gift from Dr. Jean Zhao. ST-HA-FLAG was also cloned in pBABE-puro-IRES-GFP (obtained from Addgene # 14430). PyST-Cdt1 and Geminin degron constructs were cloned by swapping PyST for SV40ST in the MSCV-puro-SV40-Cdt1/Geminin plasmids generated in Dr. David Livingston's lab. pRXTN[50] plasmid was a gift from Dr. James Iglehart.

Cell culture, retroviral and lentiviral infections

U2OS cells, U2OS ddp53 cells (dominant negative p53), HeLa cells, NIH 3T3 cells and H1299 cells were grown in DMEM medium supplemented with 10% FBS and antibiotics (penicillin and streptomycin) at 5% CO_2. Viral infections were performed as described in Andrabi et al 2007, in a BSL2 tissue culture facility. MCF10 A cells were cultured in

DMEM/F12 (1:1) with 0.5%FBS, 10 ng/ml hEGF, 0.5 μg/ml hydrocortisone, 10 μg/ml insulin and 10 μg/ml cholera toxin.

Regulated expression of small T antigen

pTREX-PyST U2OS cells were obtained by standard lentiviral infection as described above. PyST was expressed as a fusion protein with tandem FLAG and HA tags at its C- terminus. ST expression was induced by the addition of doxycycline (0.1- 1 μg/ml) to these cells.

Immunofluorescence and live cell imaging

The cells were either fixed with 4% paraformaldehyde in PBS or with ice-cold methanol. Cells were washed with PBS and permeabilized with 0.3% Triton X-100 in PBS and blocked with blocking buffer (1X PBS/5% normal goat serum/0.3% Triton X-100) for 1 hr. Chromosome spreads were prepared and categorized as described[51]. For staining, cells were incubated overnight with the appropriate primary antibody at 4°C. Subsequently, cells were washed with PBS, and incubated with fluorescent antibody (1:10,000 for FITC/TRIT-C antibodies and 1:1000 for Alexa Fluor antibodies in blocking buffer) at room temperature for 1-2 hours. Coverslips were washed 3× with PBS and mounted on glass slides with DAPI or Hoechst 33342 containing mounting medium (Vectashield from Vector laboratories) or Prolong Gold (Invitrogen) and visualized using a Zeiss or Nikon TE2000-U epifluorescence microscope with appropriate filters.

For live cell imaging, pTREX-PyST U2OS cells were infected with retroviruses generated with a GFP-tagged Histone 2B cDNA construct (a gift from Dr. Jean Zhao's lab at DFCI). Stable cells were then cultured in 35 mm Mattek tissue culture glass dishes and imaged with the Zeiss epifluorescence microscope equipped with a heating chamber and incubator (37°C). 5% CO_2 was fed via a humidifying chamber. Time-lapse imaging captured 1 image every 3 minutes. Movies were made at 5 frames per second using Zeiss Axiovision software.

Western blotting

For Western blotting, equal number of cells were seeded in 6 well dishes and the samples were extracted by directly boiling with 2× Laemmli sample buffer. In certain cases, cells were lysed with 50 mM Tris (pH 7.4), 150 mM NaCl, 1mM EDTA, 10% glycerol, 0.5% NP-40 and protease inhibitors (Roche, complete mini tablets) at 4°C for 30 minutes, followed by centrifugation at 14000 rpm at 4°C. Proteins were separated using SDS PAGE, and then transferred to 0.2 or 0.45 μM nitrocellulose membranes. The membranes were blocked either with 5% BSA or 5% milk in 1X TBST. Primary antibodies were incubated overnight at 4°C, washed 3× with 1X TBST and then incubated with Odyssey secondary antibodies (1:10,000) for 90 minutes at room temperature. The blots were subsequently washed 2× with TBST and once with TBS and developed with an Odyssey infrared scanner.

DNA laddering and Cell Cycle analysis by FACS

DNA isolation for chromosomal fragmentation was performed as described by Chen et al [52]. Cell cycle analysis was performed as described in Andrabi et al., 2007 and data were analyzed by ModFit.

Crystal violet staining

Equal numbers of cells expressing either empty vector or PyST were plated in 6 cm culture dishes and allowed to grow for a 3-4 days, washed once with PBS, and fixed with 100% ethanol for 15 minutes. Fixed cells were then stained with 0.1% crystal violet for 30 minutes. Alternatively, for experiments involving staining quantification, cells were fixed with 10% acetic acid + 10% ethanol fix solution and then stained with 0.4% crystal violet in 20% ethanol solution. In either case, the staining solution was discarded and the plates were washed with distilled water and dried. The dye was extracted with 10% acetic acid solution and quantified using a microplate spectrophotometer at 595 nm.

Supplementary Material

Refer to Web version on PubMed Central for supplementary material.

Acknowledgments

This work was supported by an NIH PO1 grant CA50661 to T.M.R, B.S.S and D.M.L and an RO1 grant to T.M.R (CA30002) and B.S.S (CA34722) and a Ramalingaswami fellowship and a CREST fellowship to S.A. J.M.G.H. is supported by the Association for International Cancer Research and is a Scholar of the Leukemia and Lymphoma Society. We thank Drs. Jennifer Spangle and Meera Bhanu for their helpful comments on this manuscript.

References

1. Cheng J, DeCaprio JA, Fluck MM, Schaffhausen BS. Cellular transformation by Simian Virus 40 and Murine Polyoma Virus T antigens. Semin Cancer Biol. 2009; 19:218–228. [PubMed: 19505649]
2. Lane DP, Crawford LV. T antigen is bound to a host protein in SV40-transformed cells. Nature. 1979; 278:261–263. [PubMed: 218111]
3. Linzer DI, Levine AJ. Characterization of a 54K dalton cellular SV40 tumor antigen present in SV40-transformed cells and uninfected embryonal carcinoma cells. Cell. 1979; 17:43–52. [PubMed: 222475]
4. Whitman M, Kaplan DR, Schaffhausen B, Cantley L, Roberts TM. Association of phosphatidylinositol kinase activity with polyoma middle-T competent for transformation. Nature. 1985; 315:239–242. [PubMed: 2987699]
5. Pallas DC, Shahrik LK, Martin BL, Jaspers S, Miller TB, Brautigan DL, et al. Polyoma small and middle T antigens and SV40 small t antigen form stable complexes with protein phosphatase 2A. Cell. 1990; 60:167–176. [PubMed: 2153055]
6. Mullane KP, Ratnofsky M, Cullere X, Schaffhausen B. Signaling from polyomavirus middle T and small T defines different roles for protein phosphatase 2A. Mol Cell Biol. 1998; 18:7556–7564. [PubMed: 9819441]
7. Janssens V, Rebollo A. The role and therapeutic potential of Ser/Thr phosphatase PP2A in apoptotic signalling networks in human cancer cells. Curr Mol Med. 2012; 12:268–287. [PubMed: 22300139]
8. Janssens V, Goris J. Protein phosphatase 2A: a highly regulated family of serine/threonine phosphatases implicated in cell growth and signalling. Biochem J. 2001; 353:417–439. [PubMed: 11171037]
9. Janssens V, Goris J, Van Hoof C. PP2A: the expected tumor suppressor. Curr Opin Genet Dev. 2005; 15:34–41. [PubMed: 15661531]
10. Lechward K, Awotunde OS, Swiatek W, Muszynska G. Protein phosphatase 2A: variety of forms and diversity of functions. Acta Biochim Pol. 2001; 48:921–933. [PubMed: 11996003]
11. Seshacharyulu P, Pandey P, Datta K, Batra SK. Phosphatase: PP2A structural importance, regulation and its aberrant expression in cancer. Cancer Lett. 2013; 335:9–18. [PubMed: 23454242]

12. Sents W, Ivanova E, Lambrecht C, Haesen D, Janssens V. The biogenesis of active protein phosphatase 2A holoenzymes: a tightly regulated process creating phosphatase specificity. FEBS J. 2013; 280:644–661. [PubMed: 22443683]
13. Schonthal AH. Role of serine/threonine protein phosphatase 2A in cancer. Cancer Lett. 2001; 170:1–13. [PubMed: 11448528]
14. Zhou J, Pham HT, Walter G. The formation and activity of PP2A holoenzymes do not depend on the isoform of the catalytic subunit. J Biol Chem. 2003; 278:8617–8622. [PubMed: 12506124]
15. Andrabi S, Hwang JH, Choe JK, Roberts TM, Schaffhausen BS. Comparisons between murine polyomavirus and Simian virus 40 show significant differences in small T antigen function. J Virol. 2011; 85:10649–10658. [PubMed: 21835797]
16. Andrabi S, Gjoerup OV, Kean JA, Roberts TM, Schaffhausen B. Protein phosphatase 2A regulates life and death decisions via Akt in a context-dependent manner. Proc Natl Acad Sci U S A. 2007; 104:19011–19016. [PubMed: 18006659]
17. Zhu ZY, Veldman GM, Cowie A, Carr A, Schaffhausen B, Kamen R. Construction and functional characterization of polyomavirus genomes that separately encode the three early proteins. J Virol. 1984; 51:170–180. [PubMed: 6328036]
18. Zheng B, Woo CF, Kuo JF. Mitotic arrest and enhanced nuclear protein phosphorylation in human leukemia K562 cells by okadaic acid, a potent protein phosphatase inhibitor and tumor promoter. J Biol Chem. 1991; 266:10031–10034. [PubMed: 1645333]
19. Toyoshima F, Nishida E. Spindle orientation in animal cell mitosis: roles of integrin in the control of spindle axis. J Cell Physiol. 2007; 213:407–411. [PubMed: 17654475]
20. Sharp-Baker H, Chen RH. Spindle checkpoint protein Bub1 is required for kinetochore localization of Mad1, Mad2, Bub3, and CENP-E, independently of its kinase activity. J Cell Biol. 2001; 153:1239–1250. [PubMed: 11402067]
21. Taylor SS, Hussein D, Wang Y, Elderkin S, Morrow CJ. Kinetochore localisation and phosphorylation of the mitotic checkpoint components Bub1 and BubR1 are differentially regulated by spindle events in human cells. J Cell Sci. 2001; 114:4385–4395. [PubMed: 11792804]
22. Kwiatkowski N, Jelluma N, Filippakopoulos P, Soundararajan M, Manak MS, Kwon M, et al. Small-molecule kinase inhibitors provide insight into Mps1 cell cycle function. Nat Chem Biol. 2010; 6:359–368. [PubMed: 20383151]
23. Sakaue-Sawano A, Kurokawa H, Morimura T, Hanyu A, Hama H, Osawa H, et al. Visualizing spatiotemporal dynamics of multicellular cell-cycle progression. Cell. 2008; 132:487–498. [PubMed: 18267078]
24. Marusyk A, Wheeler LJ, Mathews CK, DeGregori J. p53 mediates senescence-like arrest induced by chronic replicational stress. Mol Cell Biol. 2007; 27:5336–5351. [PubMed: 17515610]
25. Blagosklonny MV, Darzynkiewicz Z. Cyclotherapy: protection of normal cells and unshielding of cancer cells. Cell Cycle. 2002; 1:375–382. [PubMed: 12548008]
26. Schaffhausen BS, Roberts TM. Lessons from polyoma middle T antigen on signaling and transformation: A DNA tumor virus contribution to the war on cancer. Virology. 2009; 384:304–316. [PubMed: 19022468]
27. Daum JR, Potapova TA, Sivakumar S, Daniel JJ, Flynn JN, Rankin S, et al. Cohesion fatigue induces chromatid separation in cells delayed at metaphase. Curr Biol. 2011; 21:1018–1024. [PubMed: 21658943]
28. Kitajima TS, Sakuno T, Ishiguro K, Iemura S, Natsume T, Kawashima SA, et al. Shugoshin collaborates with protein phosphatase 2A to protect cohesin. Nature. 2006; 441:46–52. [PubMed: 16541025]
29. Tang Z, Shu H, Qi W, Mahmood NA, Mumby MC, Yu H. PP2A is required for centromeric localization of Sgo1 and proper chromosome segregation. Dev Cell. 2006; 10:575–585. [PubMed: 16580887]
30. Riedel CG, Katis VL, Katou Y, Mori S, Itoh T, Helmhart W, et al. Protein phosphatase 2A protects centromeric sister chromatid cohesion during meiosis I. Nature. 2006; 441:53–61. [PubMed: 16541024]

31. Dai J, Kateneva AV, Higgins JM. Studies of haspin-depleted cells reveal that spindle-pole integrity in mitosis requires chromosome cohesion. J Cell Sci. 2009; 122:4168–4176. [PubMed: 19910498]
32. Foley EA, Maldonado M, Kapoor TM. Formation of stable attachments between kinetochores and microtubules depends on the B56-PP2A phosphatase. Nat Cell Biol. 2011; 13:1265–1271. [PubMed: 21874008]
33. Zhu M, Settele F, Kotak S, Sanchez-Pulido L, Ehret L, Ponting CP, et al. MISP is a novel Plk1 substrate required for proper spindle orientation and mitotic progression. J Cell Biol. 2013; 200:773–787. [PubMed: 23509069]
34. Yang CS, Vitto MJ, Busby SA, Garcia BA, Kesler CT, Gioeli D, et al. Simian virus 40 small t antigen mediates conformation-dependent transfer of protein phosphatase 2A onto the androgen receptor. Mol Cell Biol. 2005; 25:1298–1308. [PubMed: 15684382]
35. Yang SI, Lickteig RL, Estes R, Rundell K, Walter G, Mumby MC. Control of protein phosphatase 2A by simian virus 40 small-t antigen. Mol Cell Biol. 1991; 11:1988–1995. [PubMed: 1706474]
36. Scheidtmann KH, Mumby MC, Rundell K, Walter G. Dephosphorylation of simian virus 40 large-T antigen and p53 protein by protein phosphatase 2A: inhibition by small-t antigen. Mol Cell Biol. 1991; 11:1996–2003. [PubMed: 1848668]
37. Kawabe T. G2 checkpoint abrogators as anticancer drugs. Mol Cancer Ther. 2004; 3:513–519. [PubMed: 15078995]
38. Neviani P, Santhanam R, Oaks JJ, Eiring AM, Notari M, Blaser BW, et al. FTY720, a new alternative for treating blast crisis chronic myelogenous leukemia and Philadelphia chromosome-positive acute lymphocytic leukemia. J Clin Invest. 2007; 117:2408–2421. [PubMed: 17717597]
39. Hwang JH, Jiang T, Kulkarni S, Faure N, Schaffhausen BS. Protein phosphatase 2A isoforms utilizing Abeta scaffolds regulate differentiation through control of Akt protein. J Biol Chem. 2013; 288:32064–32073. [PubMed: 24052256]
40. Honkanen RE, Golden T. Regulators of serine/threonine protein phosphatases at the dawn of a clinical era? Curr Med Chem. 2002; 9:2055–2075. [PubMed: 12369870]
41. Swingle M, Ni L, Honkanen RE. Small-molecule inhibitors of ser/thr protein phosphatases: specificity, use and common forms of abuse. Methods Mol Biol. 2007; 365:23–38. [PubMed: 17200551]
42. Gaillard S, Fahrbach KM, Parkati R, Rundell K. Overexpression of simian virus 40 small-T antigen blocks centrosome function and mitotic progression in human fibroblasts. J Virol. 2001; 75:9799–9807. [PubMed: 11559813]
43. Gjoerup O, Zaveri D, Roberts TM. Induction of p53-independent apoptosis by simian virus 40 small t antigen. J Virol. 2001; 75:9142–9155. [PubMed: 11533178]
44. Li S, Brignole C, Marcellus R, Thirlwell S, Binda O, McQuoid MJ, et al. The adenovirus E4orf4 protein induces G2/M arrest and cell death by blocking protein phosphatase 2A activity regulated by the B55 subunit. J Virol. 2009; 83:8340–8352. [PubMed: 19535438]
45. Li S, Szymborski A, Miron MJ, Marcellus R, Binda O, Lavoie JN, et al. The adenovirus E4orf4 protein induces growth arrest and mitotic catastrophe in H1299 human lung carcinoma cells. Oncogene. 2009; 28:390–400. [PubMed: 18955965]
46. Moule MG, Collins CH, McCormick F, Fried M. Role for PP2A in ARF signaling to p53. Proc Natl Acad Sci U S A. 2004; 101:14063–14066. [PubMed: 15383668]
47. O'Shea CC, Fried M. Modulation of the ARF-p53 pathway by the small DNA tumor viruses. Cell Cycle. 2005; 4:449–452. [PubMed: 15738654]
48. Blagosklonny MV. Mitotic arrest and cell fate: why and how mitotic inhibition of transcription drives mutually exclusive events. Cell Cycle. 2007; 6:70–74. [PubMed: 17245109]
49. Castedo M, Perfettini JL, Roumier T, Andreau K, Medema R, Kroemer G. Cell death by mitotic catastrophe: a molecular definition. Oncogene. 2004; 23:2825–2837. [PubMed: 15077146]
50. Kochupurakkal BS, Iglehart JD. Nourseothricin N-acetyl transferase: a positive selection marker for mammalian cells. PLoS One. 2013; 8:e68509. [PubMed: 23861913]
51. Dai J, Sullivan BA, Higgins JM. Regulation of mitotic chromosome cohesion by Haspin and Aurora B. Dev Cell. 2006; 11:741–750. [PubMed: 17084365]
52. Chen HH, Zhao S, Song JG. TGF-beta1 suppresses apoptosis via differential regulation of MAP kinases and ceramide production. Cell Death Differ. 2003; 10:516–527. [PubMed: 12728250]

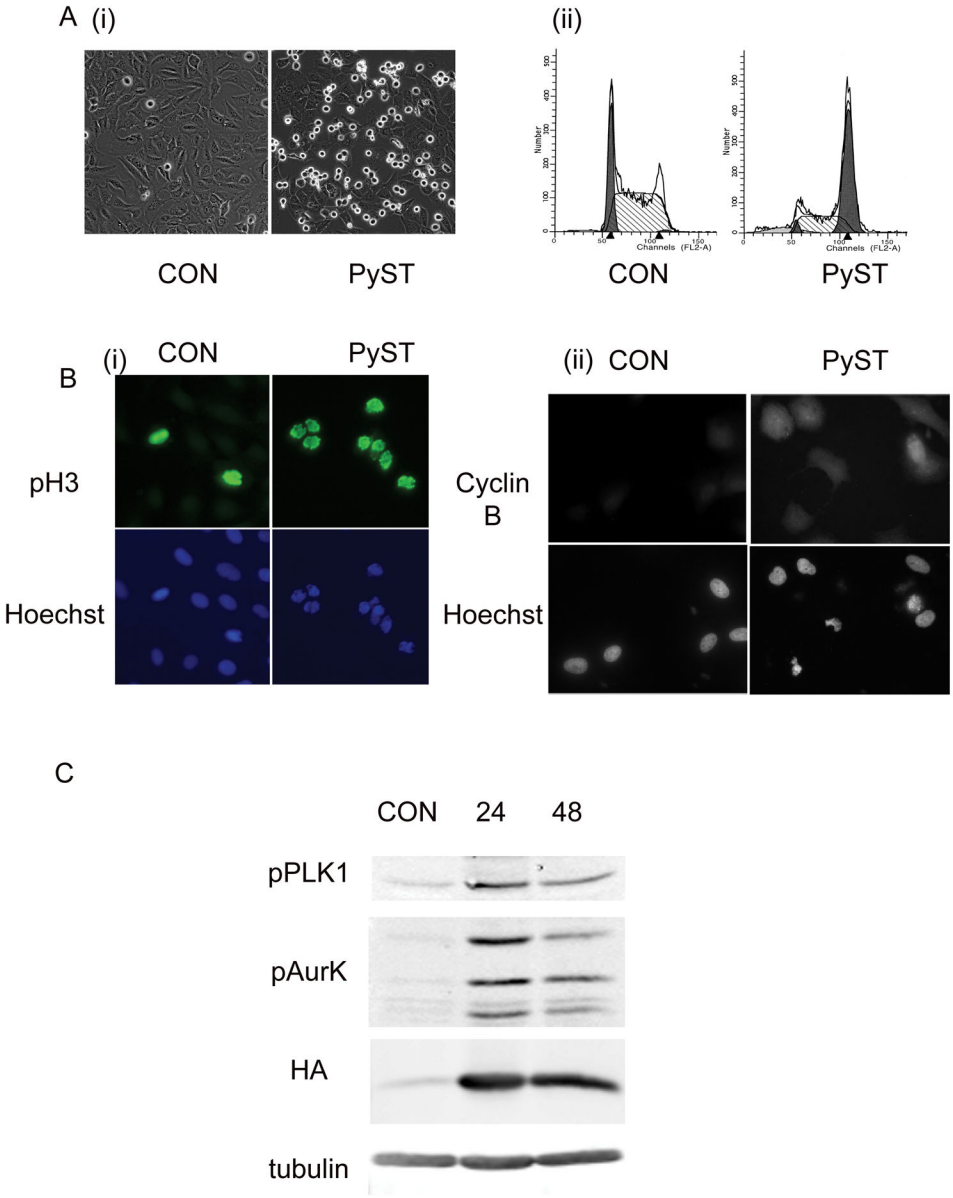

Figure 1. Polyoma small T antigen (PyST) triggers G2/M block in U2OS cells

(Ai) Phase contrast micrographs of PyST expressing cells (24h after PyST induction) and control cells. PyST expressing cells are more rounded in shape/appearance than the control cells. (Aii) Control cells and PyST expressing cells (30h after PyST induction) were fixed and stained with propidium iodide and cell cycle states were analyzed by FACS. 10,000 cells per condition were analyzed for FACS. Representative histograms from one of three such experiment are shown. Control cells have a normal cell cycle distribution while the majority of the ST expressing cells were in the G2 or M phases. (B) Fluorescence micrographs of phosphohistone (Bi) or cyclin B (Bii) in control cells or PyST expressing cells indicate that PyST expressing cells have higher proportions of mitotic cells. (C) PyST expressing cells have higher levels of mitotic markers. Total cell lysates were prepared from control cells and from cells expressing PyST for 24h or 48h post dox treatment. PyST

expressing cells had higher levels of pPLK1 and phospho aurora kinases. PyST expression was measured with an HA tag antibody. Tubulin was used as the loading control.

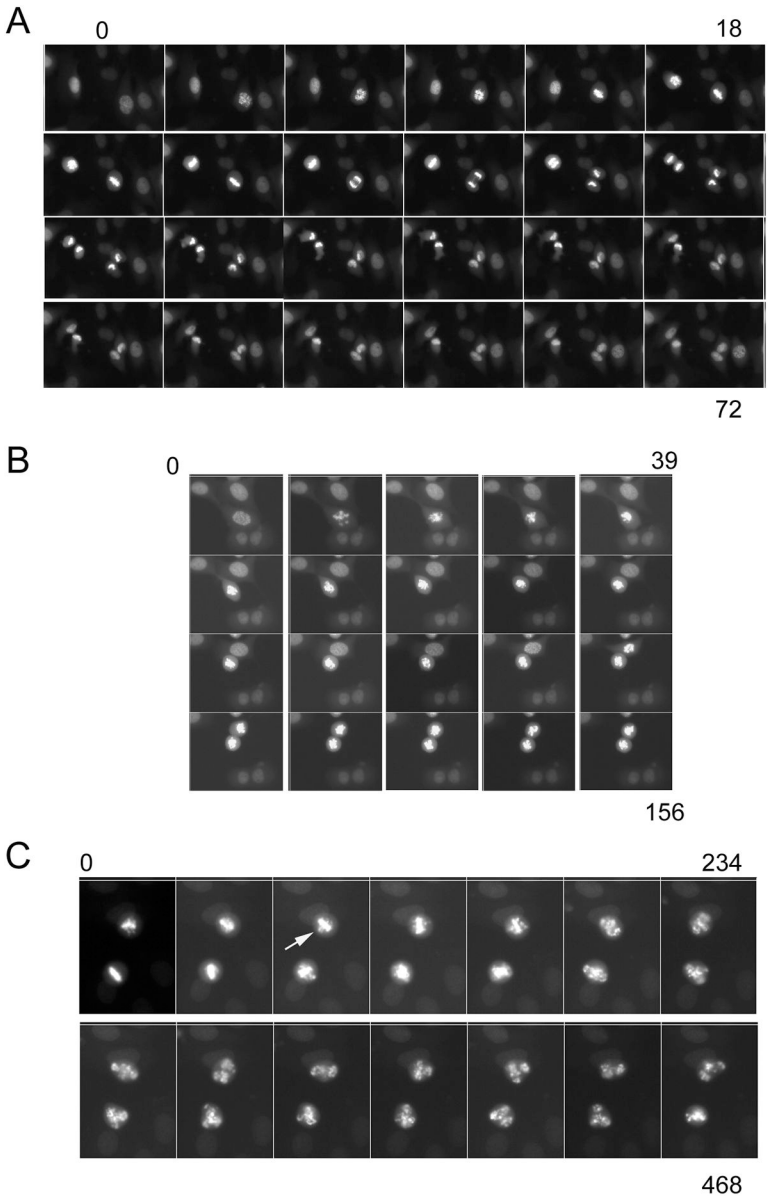

Figure 2. PyST expression triggers mitotic arrest

Live cell imaging of GFP-tagged H2B expressing control U2OS cells (A, movie 1), PyST expressing cells (B & C; movies 2 & 3). (A) Control cells divided normally with cells spending less than 60 minutes in mitosis. (B) PyST expressing cells were arrested in a prometaphase-like state. (C) Misaligned chromosomes are indicated with white arrowheads. Even in cells with aligned chromosomes (panel C bottom cell), cells, after a brief attempt to align their chromosomes, reverted to prometaphase like state. Atleast three trials per condition were performed. Representative movies are shown.

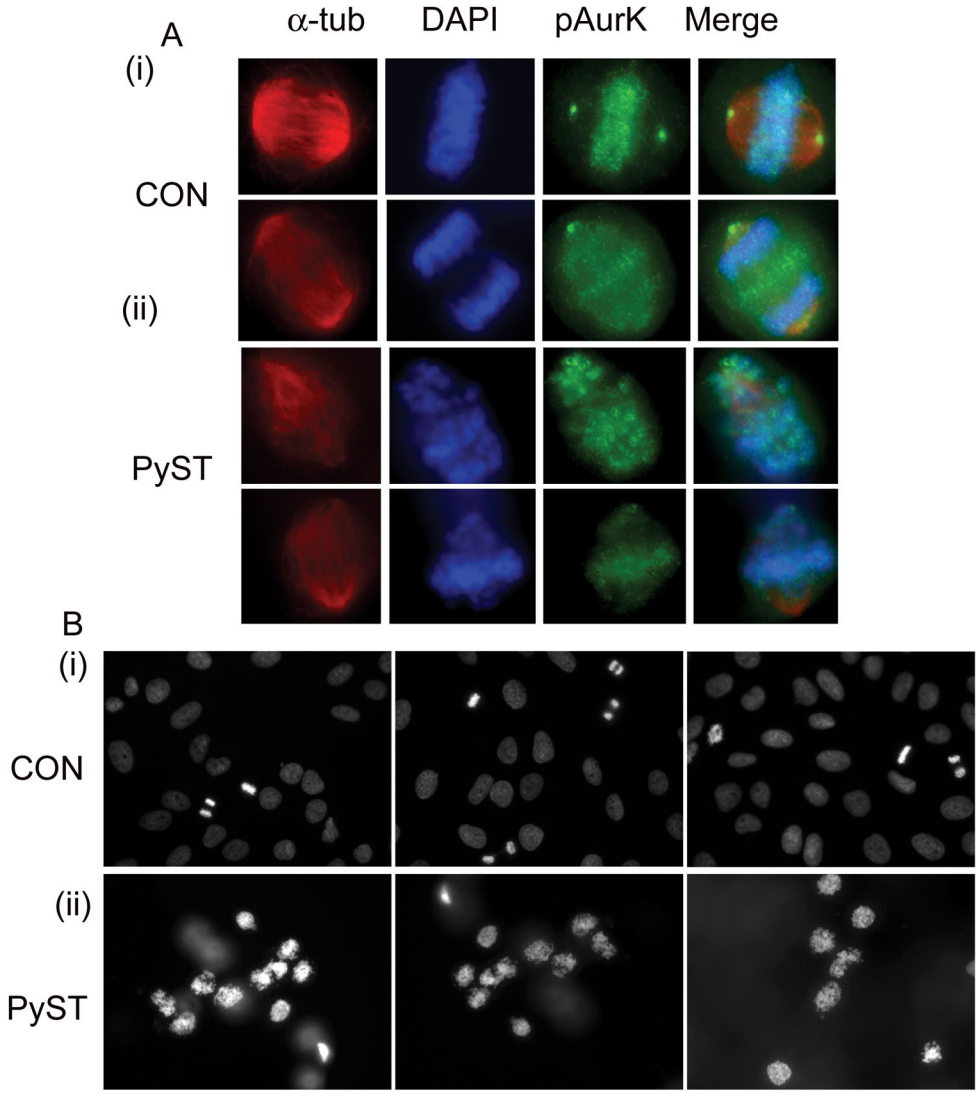

	prometaphase	metaphase	ana&telophase
Control(n=605)	34	34	32
PyST (n=683)	90	10	1

Figure 3. A majority of the PyST expressing cells were observed to be in the prometaphase stage

(Ai,ii) Phospho aurora staining confirmed that the PyST expressing cells were in mitosis. Control cells or PyST expressing cells (24h induction) were fixed and stained with anti-pan phospho aurora kinase (Phospho-aurora A (Thr288)/aurora B (Thr232)/aurora C (Thr198)) and tubulin antibodies followed by incubation with corresponding FITC/TRITC secondary antibodies. The phospho aurora staining was found to be associated with the mitotic poles and the chromosomes in both the control and PyST cells. The cells were counterstained with DAPI. (Bi,ii) Control cells and PyST- expressing cells analyzed with epifluorescence microscopy. The vast majority of the control cells were in interphase and a few cells were found to be in each of the other different mitotic states. In contrast, upon PyST expression, there was an increased prevalence of mitotic cells with PyST expression and most of the

cells were in a prometaphase-like state, with almost none of the cells in the later stages of mitosis. Results tabulated from counting mitotic cells in three such experiments are shown.

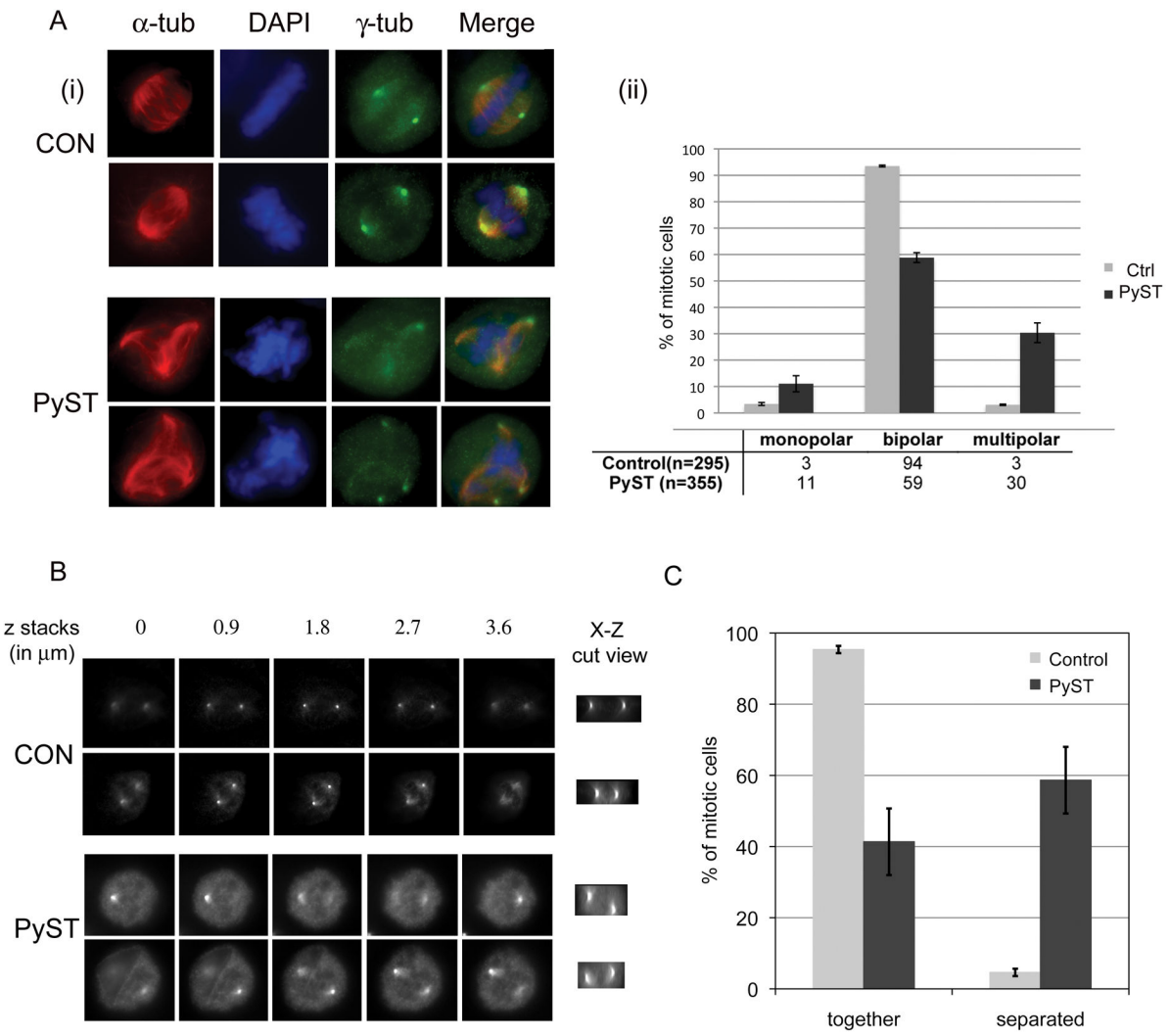

Figure 4. PyST expressing cells exhibit aberrant spindle pole formation and loss of cohesion

(A) Control cells and PyST expressing cells analyzed with epifluorescence microscopy revealed that there was an increase in the incidence of multipolar spindle formation in PyST expressing cells. Cells were fixed and stained with anti- alpha- tubulin and anti-gamma tubulin followed by corresponding FITC/TRITC secondary antibodies (Ai) or Alexa 488 and 568 secondary antibodies (Aii). Cells were counterstained with DAPI. Quantification from three such experiments is plotted in Aii. Control cells were mostly bipolar whereas PyST expressing cells showed an increased prevalence of multipolar spindles and decreased levels of bipolar spindle formation. (B) Z stacks of anti-gamma tubulin staining in control cells and PyST expressing cells imaged at 0.3 micron intervals. Representative images at 0.9 micron intervals are shown. (C) Categorization of mitotic chromosome spreads from control U2OS and PyST-expressing cells reveals defects in chromosome cohesion upon PyST expression. Means +/- SD are shown (n=4). At least 50 cells were examined in each replicate. See also See also Supplementary Figure 4.

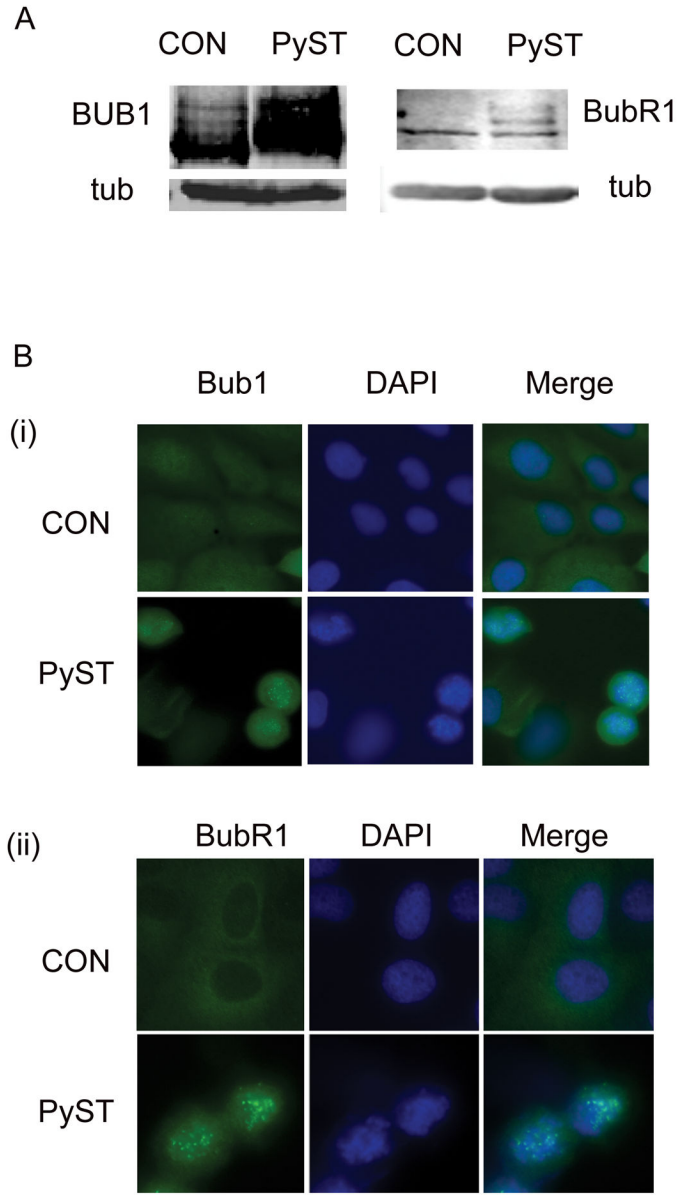

Figure 5. PyST expression triggers spindle assembly checkpoint activation

To determine the status of the spindle checkpoint, the phosphorylation patterns of Bub1 and BubR1 were analyzed by Western blotting (A). PyST expressing cells had increased levels of slowly migrating phosphorylated Bub1 and BubR1, indicating that the SAC is active. Cells were also stained with anti-Bub1 (Bi) or anti-BubR1 (Bii) followed by FITC/Alexa 488 secondary antibodies for epifluorescence micrographs. PyST expressing cells had Bub1/BubR1 staining associated with their kinetochores. Representative micrographs from one of two such experiments are shown.

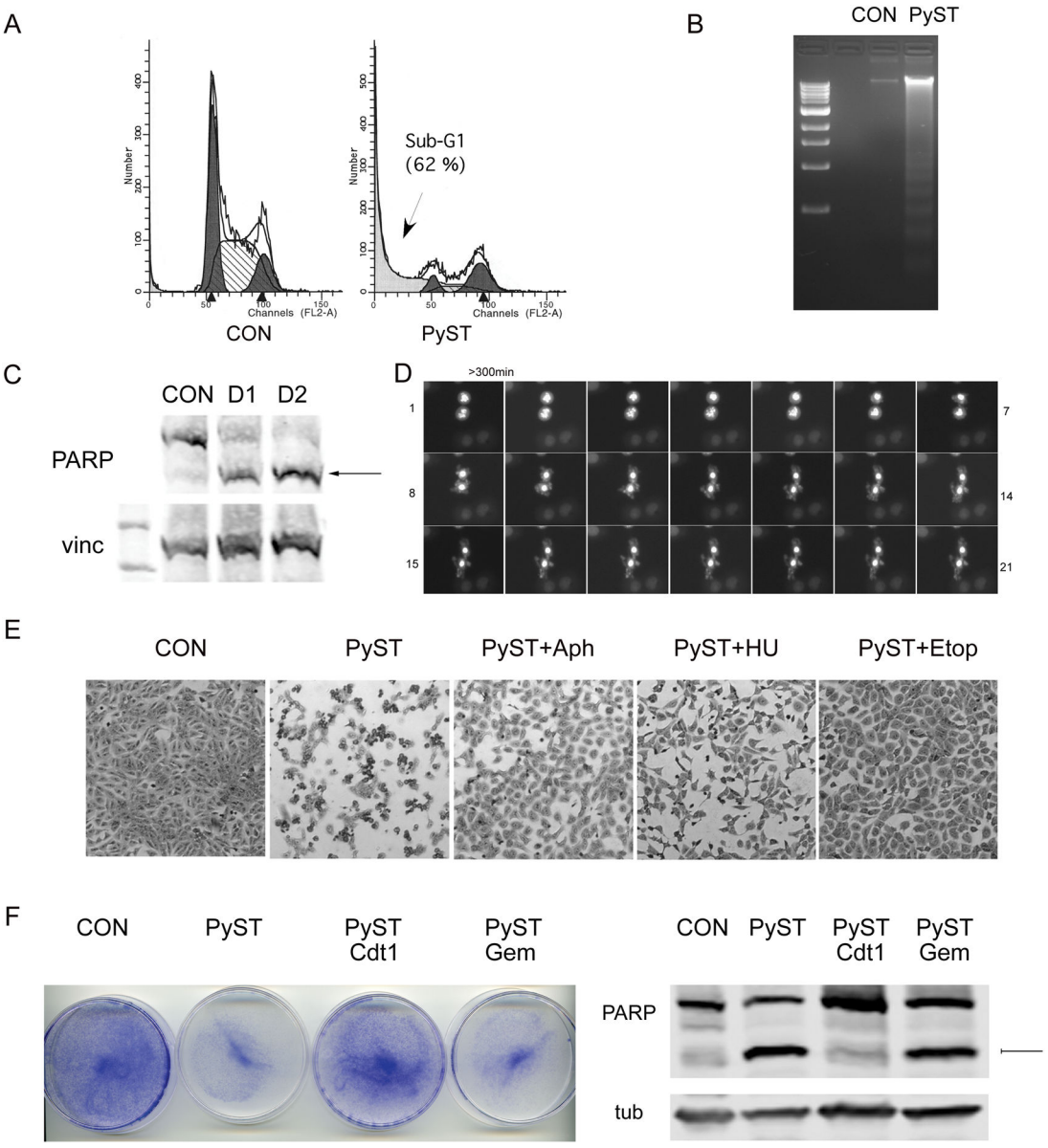

Figure 6. Characterizing cell death triggered by the regulated expression of PyST

(A) Control cells and PyST expressing cells were fixed and stained with propidium iodide and cell death was measured by FACS analysis. 10,000 cells per condition were analyzed for FACS. Control cells exhibited a normal cell cycle distribution with less than 3% of the cells in the subG1 phase while, after a 40 h induction, a majority of the PyST expressing cells were in the sub G1 phase. Arrow denotes sub-G1 group. (B) DNA laddering in PyST expressing cells and control cells. Equivalent amounts of DNA extracted from control and PyST expressing were loaded on a 2% agarose gel, electrophoresed and stained with ethidium bromide. (C) PyST triggers apoptosis. Western blotting for PARP in lysates prepared from control cells and cells expressing PyST for 24 h (D1) or 48 h (D2). Vinculin was used as the loading control. Arrow denotes cleaved PARP. (D) Prolonged mitotic arrest leads to mitotic catastrophe mediated cell death. Time-lapse imaging of PyST (GFP-H2B

expressing) expressing cells indicate that the cells die in mitosis. This is evident from the observation of cell shrinking and membrane blebbing. A representative movie from one of three such experiments is shown (movie 5). (E) Cell cycle progression inhibitors protect the cells from PyST mediated cell death. Control cells or PyST expressing cells (40 h of dox induction) were treated with aphidicolin (5 μM), etoposide (1.25 μM), hydroxyurea (1 mM) or vehicle control for 36 h (starting after 4 h of PyST induction) and were fixed and stained with crystal violet. (F) Retroviral overexpression of PyST and PyST-Geminin triggered cell death in U2OS cells. Cell density was assessed by crystal violet staining 2-3 days after retroviral transduction. Western blotting for PARP in lysates prepared from control cells and cells expressing PyST/PyST-Cdt1/PyST-Geminin for 50 h. Arrow denotes cleaved PARP. Tubulin was used as the loading control.

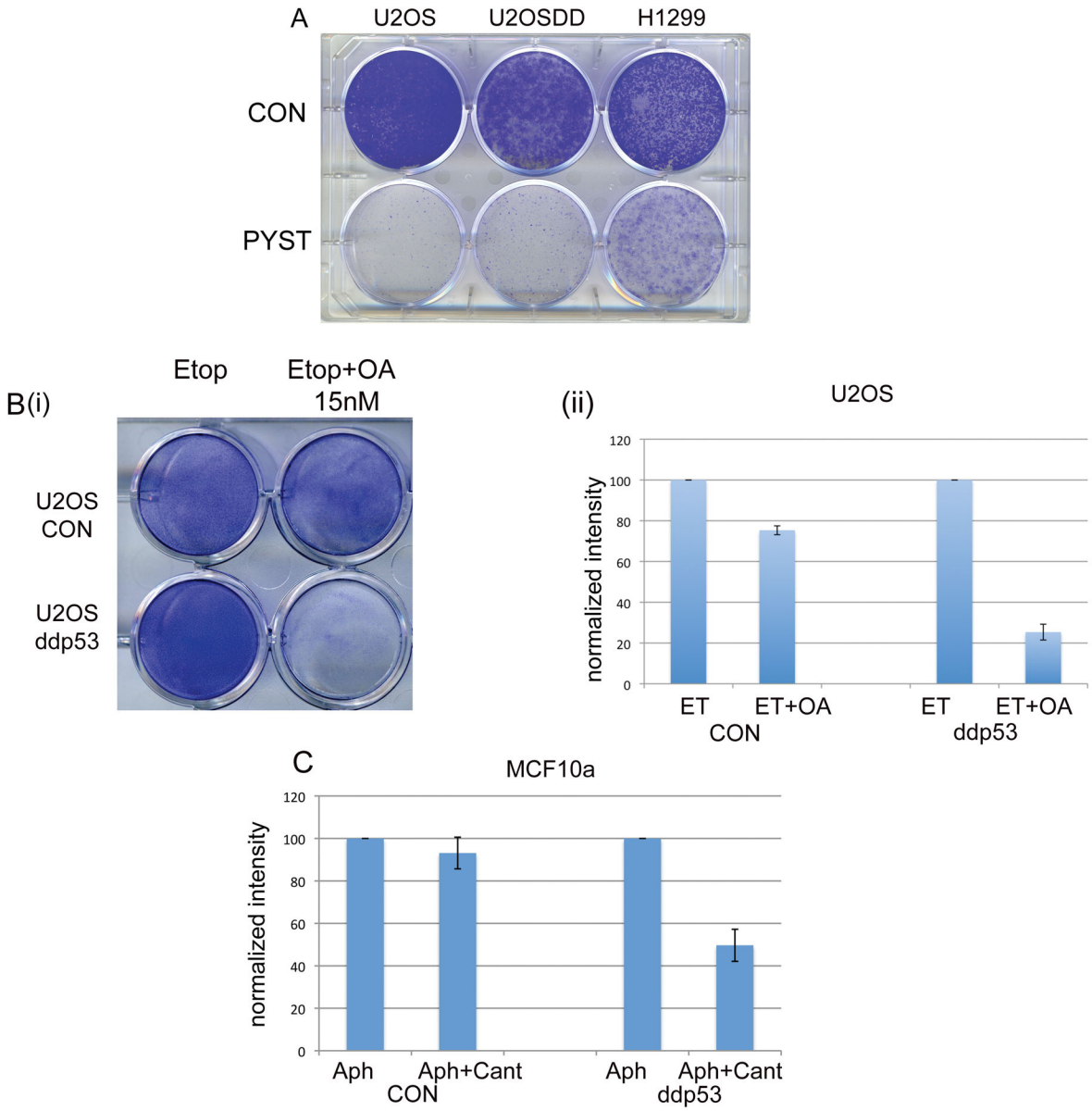

Figure 7. PyST mediated cell death is independent of p53 status and PP2A inhibition could be used to selectively kill p53 deregulated cancer cells

p53 is dispensable in PyST induced cell death. (A) Retroviral overexpression of PyST triggered cell death in H1299 cells (p53 null cell line), and in normal U2OS cells and U2OS cells engineered to overexpress dominant negative p53 (ddp53). Cell density was assessed by crystal violet staining and the end of ∼4 days after retroviral transduction. (B) PP2A inhibition coupled with etoposide (ET) treatment can be used to preferentially kill p53 deregulated cells. U2OS and ddp53 expressing U2OS cells were treated with 150 nM etoposide for 3 days, following which 15 nM OA was supplemented to the medium for 48 hours. The inhibitors were removed and cells were analyzed the following day. Cell density was assessed by crystal violet staining (B) and quantifications (crystal violet) for three independent experiments normalized to the cell density with etoposide treated conditions were plotted in panel (Bii). (C) MCF10 A and ddp53 expressing MCF10 A cells were

treated with 200 nM aphidicolin for 4-5 days, following which 1.5 μM cantharidin was supplemented to the medium for 18-20 hours. The inhibitors were removed and cells were analyzed the following day. Cell density was assessed by crystal violet staining and quantifications (crystal violet) for four independent experiments normalized to the cell density with aphidicolin-treated conditions were plotted in panel (C).